Acta Mech
DOI 10.1007/s00707-013-0944-9

Bradley T. Darrall · Gary F. Dargush · Ali R. Hadjesfandiari

Finite element Lagrange multiplier formulation for size-dependent skew-symmetric couple-stress planar elasticity

Received: 19 February 2013 / Revised: 4 June 2013

Abstract We develop a variational principle based on recent advances in couple-stress theory and the introduction of an engineering mean curvature vector as energy conjugate to the couple stresses. This new variational formulation provides a base for developing a couple-stress finite element approach. By considering the total potential energy functional to be not only a function of displacement, but of an independent rotation as well, we avoid the necessity to maintain C^1 continuity in the finite element method that we develop here. The result is a mixed formulation, which uses Lagrange multipliers to constrain the rotation field to be compatible with the displacement field. Interestingly, this formulation has the noteworthy advantage that the Lagrange multipliers can be shown to be equal to the skew-symmetric part of the force-stress, which otherwise would be cumbersome to calculate. Creating a new consistent couple-stress finite element formulation from this variational principle is then a matter of discretizing the variational statement and using appropriate mixed isoparametric elements to represent the domain of interest. Finally, problems of a hole in a plate with finite dimensions, the planar deformation of a ring, and the transverse deflection of a cantilever are explored using this finite element formulation to show some of the interesting effects of couple stress. Where possible, results are compared to existing solutions to validate the formulation developed here.

1 Introduction

It is well known that classical continuum mechanics cannot predict the behavior of materials for very small length scales. While molecular mechanics theories have certainly enjoyed some success, these approaches are only computationally feasible for collections of particles of quite limited spatial and temporal extent. This is the true motivation for developing a size-dependent continuum theory, such as the fully consistent linear elastic couple-stress theory that provides the foundation for the work here. Recent advances in couple-stress theory have resolved many of the long-standing problems that previous size-dependent continuum theories have had. In particular, some of the more important discoveries are that of the skew-symmetric nature of the couple-stress tensor and identification of mean curvature tensor as the correct second measure of deformation, as opposed to strain-gradient or other kinematic quantities that have been advocated previously. Furthermore, in this fully consistent skew-symmetric couple-stress theory, for the isotropic case, there is a single new material property,

B. T. Darrall · G. F. Dargush (✉) · A. R. Hadjesfandiari
Department of Mechanical and Aerospace Engineering, University at Buffalo,
State University of New York, Buffalo, NY 14260, USA
E-mail: gdargush@buffalo.edu

B. T. Darrall
E-mail: bdarrall@buffalo.edu

A. R. Hadjesfandiari
E-mail: ah@buffalo.edu

Published online: 27 August 2013

l, with the dimensions of length. The inclusion of couple-stress effects then becomes important for problems having characteristic geometry or loading on the order of l or smaller.

The idea of a higher-order continuum theory that included couple stress first came from Voigt [1], but the actual formulation was developed later by the Cosserat brothers in the early twentieth century [2]. Their original theory considered displacement and rotation to be separate fundamental kinematic quantities. This assumption is perfectly acceptable for approximate beam and plate theories, which represent one and two-dimensional structural elements embedded in a higher three-dimensional space. However, such is not the case for a three-dimensional continuum, and a full justification of this independence of displacement and rotation fields remains unresolved to this day.

After receiving little attention for many years the Cosserat theory was revisited, but instead of considering rotation independent of displacement, it was instead constrained to be compatible with the displacement field. These new constrained theories, which are more consistent with classical continuum approaches, became known as couple-stress theories. The original couple-stress theories, which came from Toupin [3], Mindlin and Tiersten [4] and Koiter [5], suffer from indeterminacy of the spherical part of the couple-stress tensor, as well as the inclusion of the body couple in the constitutive relation for the force-stress tensor. Consequently, these theories have been in the past referred to as inconsistent or indeterminate couple-stress theories.

Subsequent theories along these lines involving couple stress are referred to as second gradient and strain-gradient theories, which mainly differ in the measures of deformation that are considered. The measures of deformation consist of various combinations of strain, curvature, and strain-gradient. In these theories, the gradient of the rotation vector is typically considered to be the curvature tensor. The true underlying issue with these theories, however, is that the proposed measures of deformation are not the correct energy conjugate pair of the couple-stress tensor.

Soon after the development of the original couple-stress theories, people began to develop another branch of higher-order theories that more closely resembled the Cosserat theory. The idea of microrotation, a field independent of displacement, was again considered to be a fundamental kinematic quantity in an attempt to remedy the aforementioned issues with inconsistent couple-stress theories. Mindlin [6,7], Eringen [8,9], and Nowacki [10] were the first to revive these Cosserat theories that now are more commonly referred to as micropolar theories. Although these theories have been applied broadly, the inclusion of microrotation as a kinematic quantity is extraneous and does not represent a true continuum mechanics concept. If the original couple stress theories [3–5] had not encountered the obstacles mentioned above, then perhaps there would have been no need to revert to the Cosserat ideas, which stem from the consideration of lower-dimensional structural elements (e.g., beams, plates, shells) embedded in three-dimensional space. In these cases, independent rotational degrees of freedom are perfectly justified. The difficulty for micropolar theories comes in attempting to embed a full three-dimensional continuum with independent rotations into three-dimensional space.

Recently, a new couple-stress theory has been developed that resolves all issues that prior couple-stress theories have had. This new fully determinate, consistent couple-stress theory [11] uses virtual work and admissible boundary condition considerations to reveal the skew-symmetric nature of the couple-stress tensor and shows that mean curvature is in fact the correct energy conjugate measure of deformation. The variational formulations presented in the current paper will be based upon this new consistent theory. Although this consistent couple stress theory uses some elements from Mindlin and Tiersten [4] and Koiter [5], it cannot be taken as a special case; in fact, for isotropic materials, the new consistent theory is explicitly excluded based upon their definitions of the permissible material parameter ranges. Rather, these indeterminate theories can be considered as an initial inconsistent version of this final couple stress theory. Mindlin and Tiersten [4] and Koiter [5] used the gradient of the rotation as the curvature tensor. Unfortunately, this is not the proper measure of deformation energetically conjugate to couple stresses, which then creates indeterminacy in the spherical part of the couple-stress tensor, as mentioned above. For more explanation, see [12], especially Appendix A, and also [13], where the skew-symmetric character of the couple stresses is established purely from tensorial arguments.

The number of analytical solutions available for couple-stress and micropolar theories within the context of elasticity is very limited, and therefore, numerical methods must be explored. Within the field of solids and structures, the finite element method (FEM) is the most widely used numerical method, and accordingly, many couple-stress and micropolar FEM formulations have been developed, including those by Hermann [14], Wood [15], Providas and Kattis [16], Padovan [17], Shu et al. [18] and Amanatidou and Aravas [19]. All of these are mixed formulations that include additional degrees of freedom for rotation to simplify the problem, such that only C^0 continuity is required. The previous formulations mainly differ in which specific theory they

are based upon, all of which have various flaws that were mentioned previously, as well as how the rotational degrees of freedom are constrained.

In this paper, we develop a new finite element formulation based on the fully consistent couple-stress theory from [11]. We first develop a variational principle that will be used as a base for the finite element formulation. The formulation that is developed is mixed because it considers Lagrange multipliers to constrain the rotation field to be equal to one-half the curl of the displacement field. Conveniently, these Lagrange multipliers are shown to be equal to the skew-symmetric portion of the total stress tensor, which otherwise can be difficult to obtain. Creating a finite element formulation is then primarily a matter of discretizing this variational principle and choosing appropriate elements to represent the domain of interest.

Throughout this paper, standard tensor index notation will be used, where in three-dimensions, Latin subscripts range from 1 to 3 representing Cartesian coordinates x, y, and z. Repeated indices imply summation over all values for that index and commas denote partial derivatives with respect to spatial coordinates. Additionally, ε_{ijk} is the Levi-Civita alternating symbol, and δ_{ij} is the Kronecker delta. Beginning in Sect. 3, vector notation is introduced for convenience with bold face characters representing vectors and matrices.

2 Couple stress size-dependent linear elasticity

In this section, a brief overview is provided of the important concepts and relations in the recent consistent couple-stress theory for solids. The focus is primarily on the relations that are pertinent to the development of the couple-stress finite element formulation presented here. For a more detailed discussion on the theory, the reader is referred to [11].

From couple-stress theory, a general three-dimensional body under quasistatic conditions is governed throughout its volume V by the following equilibrium equations coming from linear and angular momentum balance, respectively:

$$\sigma_{ji,j} + \bar{F}_i = 0, \tag{1}$$

$$\mu_{ji,j} + \varepsilon_{ijk}\sigma_{jk} = 0, \tag{2}$$

where σ_{ji} and μ_{ji} are the force-stresses and couple stresses, respectively, while $\bar{F}_i$ represents applied body forces. The consideration of body couples is shown to be redundant in [11]. All body couple systems can be replaced by an equivalent system of body forces and surface tractions.

In addition, the body is subject to boundary conditions on the surface S. Let us assume that the natural boundary conditions take the form

$$t_i = \bar{t}_i \quad \text{on} \quad S_t, \tag{3a}$$

$$m_i = \bar{m}_i \quad \text{on} \quad S_m, \tag{3b}$$

while the essential boundary conditions can be written

$$u_i = \bar{u}_i \quad \text{on} \quad S_u, \tag{4a}$$

$$\omega_i = \bar{\omega}_i \quad \text{on} \quad S_\omega. \tag{4b}$$

Here, t_i and m_i represent the force-tractions and moment-tractions, respectively, while u_i and ω_i are the displacements and rotations, respectively, and the overbars denote the specified values. For a well-defined boundary value problem, we should have $S_t \bigcup S_u = S$, $S_t \bigcap S_u = \emptyset$ and $S_m \bigcup S_\omega = S$, $S_m \bigcap S_\omega = \emptyset$.

From the theoretical development in [11], the normal component of $\bar{m}_i$ is zero and the normal component of $\bar{\omega}_i$ cannot be specified. In general, the moment-traction m_i has only a bending effect on the boundary surface, whether or not this quantity is specified.

In general, the relations between force-stress and force-traction, and couple-stress and moment-traction can be written

$$t_i = \sigma_{ji} n_j, \tag{5a}$$

$$m_i = \mu_{ji} n_j, \tag{5b}$$

where n_i represents the outward unit normal vector to the surface S.

Regarding the kinematics, we may take the gradient of the displacement field and split it into its symmetric and skew-symmetric parts, such that

$$u_{(i,j)} = e_{ij} = \frac{1}{2}(u_{i,j} + u_{j,i}), \tag{6a}$$

$$u_{[i,j]} = \omega_{ij} = \frac{1}{2}(u_{i,j} - u_{j,i}), \tag{6b}$$

where the parenthesis around the indices represent the symmetric part of the tensor, while the square brackets indicate the skew-symmetric part of the tensor. Here, we recognize e_{ij} as the linear strain tensor and ω_{ij} as the rotation tensor, under infinitesimal deformation theory. Because ω_{ij} is a skew-symmetric tensor with three independent values, it can be represented by an axial or pseudo-vector. According to the right-hand convention, the rotation vector dual to ω_{ij} should be defined as follows:

$$\omega_i = \frac{1}{2}\varepsilon_{ijk}\omega_{kj}. \tag{7a}$$

Then, the relationship between displacement and rotation can be expressed as

$$\omega_k = \frac{1}{2}\varepsilon_{ijk}u_{j,i}. \tag{7b}$$

Taking the gradient of the rotation field and only considering the skew-symmetric contribution, we are left with the mean curvature tensor

$$\kappa_{ij} = \omega_{[i,j]} = \frac{1}{2}(\omega_{i,j} - \omega_{j,i}). \tag{8}$$

Because this mean curvature tensor is skew-symmetric, it can be represented as a polar vector through the following duality relation:

$$\kappa_i = \frac{1}{2}\varepsilon_{ijk}\kappa_{kj}. \tag{9}$$

From classical linear elasticity theories, we know that the strain contributes to the overall elastic potential energy; however, in [11], it is shown that mean curvature is the second suitable measure of deformation, which also contributes to the elastic potential energy. Indeed, it is shown in [11] that the mean curvature tensor is the energy conjugate quantity to the couple-stress tensor for a consistent couple-stress theory. Other past theories have concluded that the strain-gradient or other higher-order kinematic quantities should be considered. However, this has been shown in [11] to be incorrect by considering admissible boundary conditions and virtual work applied to an arbitrary continuum material element. The important consequence of this discovery is the skew-symmetric nature of the couple-stress tensor, which makes the theory fully determinate.

Because the couple-stress tensor is skew-symmetric, it also has a corresponding dual polar vector μ_i, where

$$\mu_i = \frac{1}{2}\varepsilon_{ijk}\mu_{kj}. \tag{10}$$

From Eq. (2), the skew-symmetric portion of the force-stress tensor is related to the couple stress by

$$\sigma_{[ji]} = -\mu_{[i,j]} = -\frac{1}{2}\left(\mu_{i,j} - \mu_{j,i}\right). \tag{11}$$

Naturally, this skew-symmetric portion can be represented as a pseudo-vector s_i as well, such that

$$s_i = \frac{1}{2}\varepsilon_{ijk}\sigma_{[kj]} \tag{12a}$$

and

$$\varepsilon_{ijk}s_k = \sigma_{[ji]}. \tag{12b}$$

For force-stress, we have the obvious decomposition

$$\sigma_{ji} = \sigma_{(ji)} + \sigma_{[ji]}, \tag{13a}$$

which, after substituting Eq. (12b), may be written

$$\sigma_{ji} = \sigma_{(ji)} + \varepsilon_{ijk} s_k. \tag{13b}$$

Furthermore, substituting Eq. (13b) into Eq. (1) and Eq. (12a) into Eq. (2) yields the following alternate relations for linear and angular momentum balance:

$$\sigma_{(ji),j} + \varepsilon_{ijk} s_{k,j} + \bar{F}_i = 0, \tag{14a}$$

$$\mu_{ji,j} + 2s_i = 0. \tag{14b}$$

Based upon the development in [11], we may write the elastic energy density for a linear, isotropic couple stress material as

$$U(e, \kappa) = \frac{1}{2} c_{ijkl} e_{ij} e_{kl} + \frac{1}{2} b_{ijkl} \kappa_{ij} \kappa_{kl}. \tag{15}$$

in terms of the tensorial strain e_{ij} and mean curvature κ_{ij}. In Eq. (15), c_{ijkl} is the standard fourth-order constitutive tensor used for classical linear elasticity theories, which in the isotropic case depends on two elastic constants, for example, the Lamé constants λ and μ. Meanwhile, b_{ijkl} is the fourth-order linear couple-stress constitutive tensor.

In the present work, we will also deal with energy conjugate mean curvature and couple-stress polar vectors. Consequently, we define the engineering mean curvature k_i, such that

$$k_i = -2\kappa_i = \varepsilon_{ijk} \kappa_{jk}. \tag{16}$$

With this definition, the components of the engineering mean curvature, k_1, k_2, and k_3, at any point P, are the mean curvature of planes parallel to the x_2x_3, x_3x_1 and x_1x_2-planes, respectively, at that point.

For the elastic energy density, we may write

$$U(e, k) = \frac{1}{2} c_{ijkl} e_{ij} e_{kl} + \frac{1}{2} b_{ij} k_i k_j \tag{17}$$

with constitutive tensor b_{ij}.

From the internal energy density Eq. (15), the constitutive relations for symmetric force-stress and couple stress can be derived, respectively, as follows:

$$\sigma_{(ji)} = \frac{\partial U}{\partial e_{ij}} = c_{ijkl} e_{kl}, \tag{18}$$

$$\mu_{ji} = \frac{\partial U}{\partial \kappa_{ij}} = b_{ijkl} \kappa_{kl}, \tag{19a}$$

while the vector form of couple stress can be related to the internal energy from Eq. (17) by

$$\mu_i = \frac{\partial U}{\partial k_i} = b_{ij} k_j \tag{19b}$$

and the two couple-stress constitutive tensors are related by

$$b_{lmrs} = \varepsilon_{ilm} \varepsilon_{jrs} b_{ij}. \tag{20}$$

Equation (19b) tells us that the couple-stress vector μ_i and engineering mean curvature vector k_i are indeed the correct energy conjugate vector quantities. This form is more convenient than in [11], where use of the dual curvature vector κ_i requires introduction of a factor of minus two within the energy conjugacy relations. This is the underlying reason for introducing k_i here, as the engineering mean curvature vector. Furthermore, the components of k_i are consistent with the usual mathematical definition of mean curvatures of the three orthogonal planes oriented with the global axes at a point.

From [11], only one additional material property, η, is necessary to form the couple stress constitutive tensor for an isotropic material. For the simple case of linear elasticity in an isotropic material, we have

$$b_{lmrs} = 4\eta \left(\delta_{lr} \delta_{ms} - \delta_{ls} \delta_{mr} \right), \tag{21}$$

$$b_{ij} = 4\eta \delta_{ij}. \tag{22}$$

Interestingly, we find that there is a characteristic length l associated with such materials, defined by the relationship

$$\frac{\eta}{\mu} = l^2. \tag{23}$$

Consequently, we expect that for the impacts of couple stress to be significant, the problem at hand must have some geometric or loading dimension of importance that is comparable in magnitude to l or perhaps smaller.

3 Couple stress variational formulation

The goal here is to develop a variational formulation for a couple-stress solid that has linear and angular momentum balances, as well as the natural boundary conditions as its resulting Euler–Lagrange equations and only requires C^0 continuity of the field variables. In order to relax continuity requirements, we consider rotation to be independent from displacement and then enforce rotation-displacement compatibility through the use of Lagrange multipliers. It is shown that this formulation has the interesting advantage that these Lagrange multipliers are equal to the skew-symmetric stress, which otherwise would be difficult to calculate. Because of these aforementioned advantages, this formulation is a very convenient starting point for developing numerical methods, specifically FEM formulations [20,21], such as the one to be presented here.

Consider the following total energy functional that includes the internal elastic energy and the potential energy from applied forces:

$$\Pi = \frac{1}{2}\int_V e_{ij}c_{ijkl}e_{kl}\,\mathrm{d}V + \frac{1}{2}\int_V \kappa_{ij}b_{ijkl}\kappa_{kl}\mathrm{d}V - \int_V u_i\bar{F}_i\mathrm{d}V - \int_{S_t} u_i\bar{t}_i\,\mathrm{d}S - \int_{S_m}\omega_i\bar{m}_i\,\mathrm{d}S. \tag{24}$$

Recall that the overbars denote applied forces and moments, which consequently are not subject to variation.

In the couple stress continuum problem, both strain and curvature are functions of the displacement field, such that

$$\Pi \equiv \Pi\left(e\left(u\right), \kappa\left(u\right), u\right). \tag{25}$$

We now can extremize this functional by taking the first variation and setting that equal to zero. However, this would require C^1 continuity of the displacement field.

Alternatively, we may consider independent displacements and rotations and then enforce the rotation-displacement compatibility constraint Eq. (7b) by incorporating Lagrange multipliers into our original energy functional prior to taking the variation. Thus, we may define a new functional

$$\tilde{\Pi} \equiv \tilde{\Pi}\left(e\left(u\right), \kappa\left(\omega\right), u, \omega, \lambda\right) \tag{26}$$

where

$$\tilde{\Pi} = \Pi + \int_V \lambda_k\left(\varepsilon_{kji}u_{i,j} - 2\omega_k\right)\mathrm{d}V \tag{27}$$

and finally

$$\begin{aligned}\tilde{\Pi} = {} & \frac{1}{2}\int_V e_{ij}c_{ijkl}e_{kl}\,\mathrm{d}V + \frac{1}{2}\int_V \kappa_{ij}b_{ijkl}\kappa_{kl}\,\mathrm{d}V + \int_V \lambda_k\left(\varepsilon_{kji}u_{i,j} - 2\omega_k\right)\,\mathrm{d}V \\ & - \int_V u_i\bar{F}_i\,\mathrm{d}V - \int_{S_t} u_i\bar{t}_i\,\mathrm{d}S - \int_{S_m}\omega_i\bar{m}_i\,\mathrm{d}S,\end{aligned} \tag{28}$$

where the components of λ_i are the Lagrange multipliers. After some maneuvers, we will show that these Lagrange multipliers λ_i are equal to the skew-symmetric stress vector s_i.

We now consider the stationarity of this functional in order to find the static equilibrium solution by equating the first variation to zero. With a bit of mathematical manipulation, we will show that the solutions emanating from this process are identical to the solutions that satisfy the governing partial differential equations for our

system, as well as the natural boundary conditions. In other words, the resulting Euler–Lagrange equations represent linear momentum balance, angular momentum balance, rotation-displacement compatibility, and both the force- and moment-traction boundary conditions.

For the stationarity of $\tilde{\Pi}$, we enforce its first variation in Eq. (28) to be zero, that is

$$\delta\tilde{\Pi} = \frac{\partial\tilde{\Pi}}{\partial u_i}\delta u_i + \frac{\partial\tilde{\Pi}}{\partial\omega_i}\delta\omega_i + \frac{\partial\tilde{\Pi}}{\partial\lambda_i}\delta\lambda_i = 0. \tag{29}$$

This can be written as

$$\begin{aligned}\delta\tilde{\Pi} = &\int_V \left(c_{ijkl}e_{kl} + \varepsilon_{kji}\lambda_k\right)\delta u_{i,j}\,\mathrm{d}V + \int_V b_{ijkl}\kappa_{kl}\delta\omega_{i,j}\,\mathrm{d}V - 2\int_V \lambda_i\delta\omega_i\,\mathrm{d}V \\ &+ \int_V \delta\lambda_k\left(\varepsilon_{kji}u_{i,j} - 2\omega_k\right)\mathrm{d}V + \int_V \delta u_i\bar{F}_i\,\mathrm{d}V - \int_{S_t}\delta u_i\bar{t}_i\,\mathrm{d}S - \int_{S_m}\delta\omega_i\bar{m}_i\,\mathrm{d}S = 0,\end{aligned} \tag{30}$$

where the symmetric character of c_{ijkl} and b_{ijkl} has been used to simplify the first and second terms. Considering the product rule, we can rewrite the first two integrals in Eq. (30), such that

$$\begin{aligned}\delta\tilde{\Pi} = &\int_V \left[\left(c_{ijkl}e_{kl} + \varepsilon_{kji}\lambda_k\right)\delta u_i\right]_{,j}\,\mathrm{d}V - \int_V \left[\left(c_{ijkl}e_{kl} + \varepsilon_{kji}\lambda_k\right)_{,j} + \bar{F}_i\right]\delta u_i\,\mathrm{d}V \\ &+ \int_V \left(b_{ijkl}\kappa_{kl}\delta\omega_i\right)_{,j}\,\mathrm{d}V - \int_V \left[\left(b_{ijkl}\kappa_{kl}\right)_{,j} + 2\lambda_i\right]\delta\omega_i\,\mathrm{d}V \\ &+ \int_V \delta\lambda_k\left(\varepsilon_{kji}u_{i,j} - 2\omega_k\right)\mathrm{d}V - \int_{S_t}\delta u_i\bar{t}_i\,\mathrm{d}S - \int_{S_m}\delta\omega_i\bar{m}_i\,\mathrm{d}S = 0.\end{aligned} \tag{31}$$

Now we apply the divergence theorem to the first and third volume integrals and obtain the relation

$$\begin{aligned}\delta\tilde{\Pi} = &\int_{S_t}\left[\left(c_{ijkl}e_{kl} + \varepsilon_{kji}\lambda_k\right)n_j - \bar{t}_i\right]\delta u_i\mathrm{d}S - \int_V \left[\left(c_{ijkl}e_{kl} + \varepsilon_{kji}\lambda_k\right)_{,j} + \bar{F}_i\right]\delta u_i\mathrm{d}V \\ &+ \int_{S_m}\left[b_{ijkl}\kappa_{kl}n_j - \bar{m}_i\right]\delta\omega_i\mathrm{d}S - \int_V \left[\left(b_{ijkl}\kappa_{kl}\right)_{,j} + 2\lambda_i\right]\delta\omega_i\mathrm{d}V + \int_V \delta\lambda_k\left(\varepsilon_{kji}u_{i,j} - 2\omega_k\right)\mathrm{d}V = 0,\end{aligned} \tag{32}$$

where the conditions $\delta u_i = 0$ on S_u and $\delta\omega_i = 0$ on S_ω have been used.

Because the variations δu_i, $\delta\omega_i$, and $\delta\lambda_i$ are independent and arbitrary in the domain V and the boundary surfaces S_t and S_m, each individual term in the integrals must vanish separately. Therefore, we have

$$\left(c_{ijkl}e_{kl} + \varepsilon_{kji}\lambda_k\right)_{,j} + \bar{F}_i = 0 \quad \text{in} \quad V, \tag{33}$$

$$\left(b_{ijkl}\kappa_{kl}\right)_{,j} + 2\lambda_i = 0 \quad \text{in} \quad V, \tag{34}$$

$$\omega_k = \frac{1}{2}\varepsilon_{ijk}u_{j,i} \quad \text{in} \quad V, \tag{35}$$

$$\bar{t}_i = \left(c_{ijkl}e_{kl} + \varepsilon_{kji}\lambda_k\right)n_j \quad \text{on} \quad S_t, \tag{36}$$

$$\bar{m}_i = b_{ijkl}\kappa_{kl}n_j \quad \text{on} \quad S_m. \tag{37}$$

Equations (33) and (34) are the equilibrium Eqs. (1) and (2), where

$$\sigma_{(ji)} = c_{ijkl}e_{kl}, \tag{38}$$

$$\sigma_{[ji]} = \lambda_k\varepsilon_{kji}, \tag{39}$$

$$\mu_{ji} = b_{ijkl}\kappa_{kl}, \tag{40}$$

$$\varepsilon_{ijk}\sigma_{jk} = 2\lambda_i. \tag{41}$$

By comparing Eqs. (41) and (12a), we obtain

$$\lambda_i = s_i \quad \text{in} \quad V. \tag{42}$$

This result is of importance theoretically and also because calculating the skew-symmetric stress otherwise would be a non-trivial task, involving higher-order derivatives.

Meanwhile, Eqs. (36) and (37) yield the natural boundary conditions Eqs. (3a) and (3b), respectively.

We have now shown that the variational principle associated with the stationarity of Eq. (28) is valid for couple stress isotropic elasticity. The solutions obtained from Eq. (29) will satisfy both linear and angular equilibrium, as well as the natural boundary conditions. Furthermore, the Lagrange multiplier vector was shown to be equal to the skew-symmetric stress vector. Note that the formulation developed here is in terms of the vector forms of rotation and skew-symmetric stress. This is for convenience and uniformity of variables; however, we could also consider the same type of formulation in terms of the respective tensor form of these variables.

4 Couple stress finite element formulation

In order to take full advantage of the recent advances in couple-stress theory reviewed here, numerical methods must be explored. Here, we develop a FEM formulation that will include couple-stress effects.

For the purpose of simplifying calculations and programming, Voigt notation is used. This means that the strain, $\boldsymbol{e}$, can be represented by a vector rather than a second-order tensor, and the constitutive tensor, $\boldsymbol{c}$, can be represented by a two-dimensional matrix rather than a fourth-order tensor. For the two-dimensional, plane-strain, linear, isotropic problems that we will explore here, we then have the following relations:

$$\boldsymbol{e} = \begin{bmatrix} e_{xx} \\ e_{yy} \\ \gamma_{xy} \end{bmatrix} = \begin{bmatrix} \frac{\partial u_x}{\partial x} \\ \frac{\partial u_y}{\partial y} \\ \frac{\partial u_x}{\partial y} + \frac{\partial u_y}{\partial x} \end{bmatrix}, \tag{43}$$

$$\boldsymbol{c} = \frac{E(1-\nu)}{(1+\nu)(1-2\nu)} \begin{bmatrix} 1 & \frac{\nu}{1-\nu} & 0 \\ \frac{\nu}{1-\nu} & 1 & 0 \\ 0 & 0 & \frac{1-2\nu}{2(1-\nu)} \end{bmatrix}, \tag{44}$$

where u_x is the component of displacement in the x-direction and u_y is the component of the displacement in the y-direction. Additionally, E is the Young's modulus, and ν is the Poisson's ratio. For plane-stress problems, the only thing that will change is c [20,21].

For planar problems, the engineering mean curvature in vector form can be written in terms of the one out of plane component of rotation explicitly as

$$\boldsymbol{k} = \begin{bmatrix} k_x \\ k_y \end{bmatrix} = \begin{bmatrix} -\frac{\partial \omega}{\partial y} \\ \frac{\partial \omega}{\partial x} \end{bmatrix}, \tag{45}$$

where $\omega = \omega_z$ and the couple-stress constitutive matrix for a linear isotropic material is

$$\boldsymbol{b} = 4\eta \begin{bmatrix} 1 & 0 \\ 0 & 1 \end{bmatrix}. \tag{46}$$

We now reconsider the variational principle developed in the preceding section. In vector notation, we have

$$\delta\tilde{\Pi} = \frac{\partial \tilde{\Pi}}{\partial \boldsymbol{u}}\delta\boldsymbol{u} + \frac{\partial \tilde{\Pi}}{\partial \boldsymbol{\omega}}\delta\boldsymbol{\omega} + \frac{\partial \tilde{\Pi}}{\partial \boldsymbol{s}}\delta\boldsymbol{s} = 0, \tag{47}$$

where

$$\tilde{\Pi} = \frac{1}{2}\int_V \boldsymbol{e}^T\boldsymbol{c}\boldsymbol{e}\,\mathrm{d}V + \frac{1}{2}\int_V \boldsymbol{k}^T\boldsymbol{b}\boldsymbol{k}\,\mathrm{d}V + \int_V (\operatorname{curl}\boldsymbol{u} - 2\boldsymbol{\omega})^T\boldsymbol{s}\,\mathrm{d}V - \int_V \boldsymbol{u}^T\bar{\boldsymbol{F}}\,\mathrm{d}V - \int_{S_t} \boldsymbol{u}^T\bar{\boldsymbol{t}}\,\mathrm{d}S - \int_{S_m} \boldsymbol{\omega}^T\bar{\boldsymbol{m}}\,\mathrm{d}S. \tag{48}$$

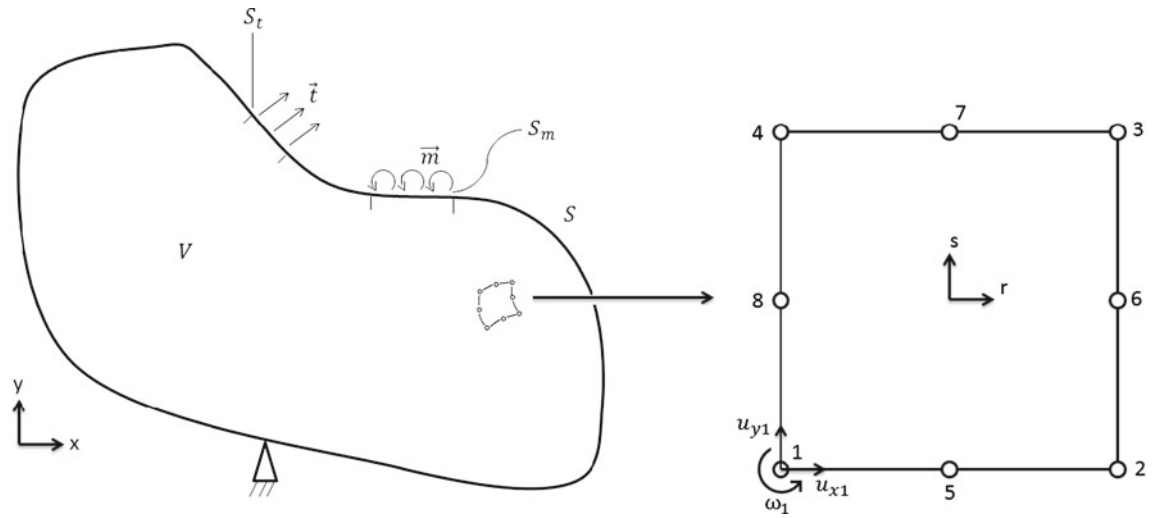

Fig. 1 General two-dimensional body and 8-node isoparametric master element

This mixed formulation has additional degrees of freedom when compared to a pure displacement based formulation, namely rotation and skew-symmetric stress, but only requires C^0 continuity for displacement.

Now consider discretizing our domain into a finite number of elements. In particular, 8-node quadratic elements are used in this formulation. The reason for not considering simpler four-node elements is that the linear elements have increased difficulty in terms of maintaining rotation-displacement compatibility when compared to higher-order elements.

Figure 1 shows a standard 8-node isoparametric quadrilateral master element. This element has natural coordinates represented by r and s, with values for each element ranging from -1 to $+1$ in either direction. In the global coordinate system, here represented in two dimensions by Cartesian coordinates x and y, our element can take on any arbitrary shape so long as the distortion of the geometry is not too extreme [20,21].

Standard serendipity quadratic shape functions $\boldsymbol{N}$ [20,21] are used in this formulation, where for completeness of presentation,

$$\boldsymbol{N}^T = \begin{bmatrix} \frac{1}{4}(1-r)(1-s) - \frac{1}{4}\left(1-s^2\right)(1-r) - \frac{1}{4}\left(1-r^2\right)(1-s) \\ \frac{1}{4}(1+r)(1-s) - \frac{1}{4}\left(1-r^2\right)(1-s) - \frac{1}{4}\left(1-s^2\right)(1+r) \\ \frac{1}{4}(1+r)(1+s) - \frac{1}{4}\left(1-r^2\right)(1+s) - \frac{1}{4}\left(1-s^2\right)(1+r) \\ \frac{1}{4}(1-r)(1+s) - \frac{1}{4}\left(1-r^2\right)(1+s) - \frac{1}{4}\left(1-s^2\right)(1-r) \\ \frac{1}{2}(1-s)\left(1-r^2\right) \\ \frac{1}{2}(1+r)\left(1-s^2\right) \\ \frac{1}{2}(1+s)\left(1-r^2\right) \\ \frac{1}{2}(1-r)\left(1-s^2\right) \end{bmatrix}. \tag{49}$$

These same shape functions $\boldsymbol{N}$ are used to interpolate both the geometric coordinates of the element as well as the displacement and rotation field variables within the element. This means that we represent the geometry of an arbitrary-shaped element in terms of the natural coordinates r and s via the following relations:

$$x \cong \boldsymbol{N}\hat{\boldsymbol{x}}, \tag{50a}$$

$$y \cong \boldsymbol{N}\hat{\boldsymbol{y}}, \tag{50b}$$

where $\hat{\boldsymbol{x}}$ and $\hat{\boldsymbol{y}}$ are the global coordinate values of nodes 1 through 8 for any particular element. We can then use these same shape functions to approximate the unknown displacement and rotation fields as follows:

$$u_x \cong \boldsymbol{N}\hat{\boldsymbol{u}}_{\boldsymbol{x}}, \tag{51a}$$
$$u_y \cong \boldsymbol{N}\hat{\boldsymbol{u}}_{\boldsymbol{y}}, \tag{51b}$$
$$\omega \cong \boldsymbol{N}\hat{\boldsymbol{\omega}}, \tag{51c}$$

with similar relations to represent the corresponding variations. In general, the hat notation is used to represent vectors containing quantities at nodes 1 through 8. For example, $\hat{\boldsymbol{\omega}}$ is a vector of length 8 containing the nodal values of planar rotation for a particular element.

For the displacements and rotations on the boundaries S_t and S_m, we use surface interpolation functions, such that

$$u_{xS_t} \cong \boldsymbol{N_S}\hat{\boldsymbol{u}}_{\boldsymbol{x}}, \tag{52a}$$
$$u_{yS_t} \cong \boldsymbol{N_S}\hat{\boldsymbol{u}}_{\boldsymbol{y}}, \tag{52b}$$
$$\omega_{S_m} \cong \boldsymbol{N_S}\hat{\boldsymbol{\omega}}. \tag{52c}$$

For a 2-d body, these surface shape functions are only one-dimensional in terms of the natural coordinates. The surface shape functions we use here are

$$\boldsymbol{N_S^T} = \begin{bmatrix} \frac{1}{2}(1-r) - \frac{1}{2}(1-r^2) \\ \frac{1}{2}(1+r) - \frac{1}{2}(1-r^2) \\ 1-r^2 \end{bmatrix}. \tag{53}$$

Next, we replace the strains and curvatures in Eq. (48) with approximate discrete representations in terms of displacements and rotations. To do this, we must introduce new matrices, the strain-displacement matrix, $\boldsymbol{B_e}$, such that

$$\boldsymbol{e} \cong \boldsymbol{B_e}\hat{\boldsymbol{u}}, \tag{54}$$

the curvature-rotation matrix, $\boldsymbol{B_k}$, such that

$$\boldsymbol{k} \cong \boldsymbol{B_k}\hat{\boldsymbol{\omega}}, \tag{55}$$

and finally the curl-displacement matrix, such that

$$\nabla \times \boldsymbol{u} \cong \boldsymbol{B_{curl}}\hat{\boldsymbol{u}}. \tag{56}$$

For the planar problems we consider in this paper, we can write out these $\boldsymbol{B}$ matrices explicitly as follows:

$$\boldsymbol{B_e} = \begin{bmatrix} \frac{\partial N_1}{\partial x} & 0 & & \frac{\partial N_8}{\partial x} & 0 \\ 0 & \frac{\partial N_1}{\partial y} & \cdots & 0 & \frac{\partial N_8}{\partial y} \\ \frac{\partial N_1}{\partial y} & \frac{\partial N_1}{\partial x} & & \frac{\partial N_8}{\partial y} & \frac{\partial N_8}{\partial x} \end{bmatrix}, \tag{57a}$$

$$\boldsymbol{B_k} = \begin{bmatrix} -\frac{\partial N_1}{\partial y} & \cdots & -\frac{\partial N_8}{\partial y} \\ \frac{\partial N_1}{\partial x} & \cdots & \frac{\partial N_8}{\partial x} \end{bmatrix}, \tag{57b}$$

$$\boldsymbol{B_{curl}} = \begin{bmatrix} -\frac{\partial N_1}{\partial y} & \frac{\partial N_1}{\partial x} & \cdots & -\frac{\partial N_8}{\partial y} & \frac{\partial N_8}{\partial x} \end{bmatrix}. \tag{57c}$$

Here $\boldsymbol{B_e}$ is a matrix of size $[3\times16]$, $\boldsymbol{B_k}$ is of size $[2\times8]$, while the matrix $\boldsymbol{B_{curl}}$ is of size $[1\times16]$. Note that $\boldsymbol{B_e}$ and $\boldsymbol{B_{curl}}$ operate on an extended displacement vector that includes both x and y components. When considering Eqs. (57a) and (57c), we have

$$\hat{\boldsymbol{u}}^T = [\hat{\boldsymbol{u}}_{\boldsymbol{x}}, \hat{\boldsymbol{u}}_{\boldsymbol{y}}] = \begin{bmatrix} \hat{u}_{x1} & \hat{u}_{y1} & \cdots & \hat{u}_{x8} & \hat{u}_{y8} \end{bmatrix}. \tag{58}$$

In all cases, the $\boldsymbol{B}$ matrices above are functions of the first derivatives of our shape functions with respect to global Cartesian coordinates x and y. Of course, in order to obtain derivatives of the shape functions with respect to global coordinates, we first take derivatives with respect to natural coordinates, r and s, and then multiply by the inverse of the Jacobian, $\boldsymbol{J}$, where

$$\boldsymbol{J} = \begin{bmatrix} \frac{\partial x}{\partial r} & \frac{\partial y}{\partial r} \\ \frac{\partial x}{\partial s} & \frac{\partial y}{\partial s} \end{bmatrix}. \tag{59}$$

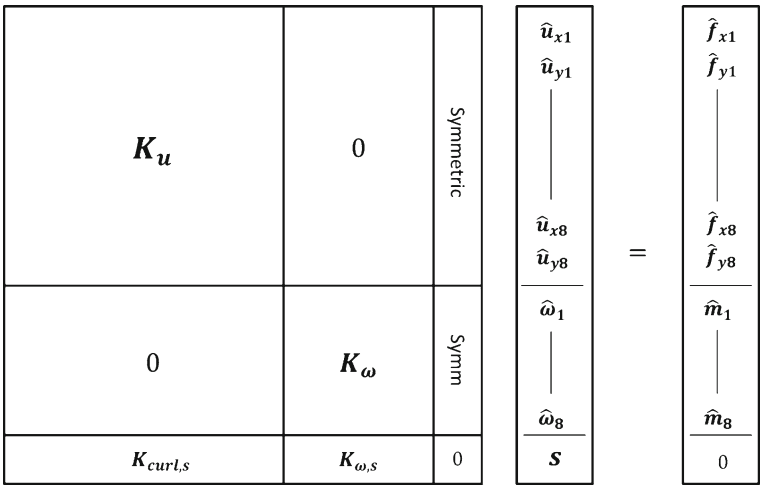

Fig. 2 Structure of resulting element equations before assembly

Finally, we must also consider the discrete approximation of the skew-symmetric stress pseudo-vector. For 2-d problems, this vector actually simplifies to one component in the out of plane direction. Further simplifying matters, we need only C^{-1} continuity in this formulation and therefore consider s to be constant throughout each element:

Now, upon substitution of the discrete representations of our variables into Eq. (48), and then taking the first variation with respect to the discrete variables, we are left with the following for each element:

$$\delta\tilde{\Pi} = \left(\delta\hat{\boldsymbol{u}}\right)^T \left[\int_V \left(\boldsymbol{B}^T \boldsymbol{c}\boldsymbol{B}\right)\hat{\boldsymbol{u}}\, J_d \mathrm{d}V + \int_V \boldsymbol{B}_{\boldsymbol{curl}}^T \boldsymbol{s}\, J_d \,\mathrm{d}V - \int_V \boldsymbol{N}^T \bar{\boldsymbol{F}} J_d \,\mathrm{d}V - \int_{S_t} \boldsymbol{N}_S^T \bar{\boldsymbol{t}}\, J_{dS}\, dS\right]$$
$$+ \left(\delta\hat{\boldsymbol{\omega}}\right)^T \left[\int_V (\boldsymbol{B}_{\boldsymbol{k}}^T \boldsymbol{b}\boldsymbol{B}_{\boldsymbol{k}})\hat{\boldsymbol{\omega}} J_d \,\mathrm{d}V + \int_V -2\boldsymbol{N}^T \boldsymbol{s}\, J_d \mathrm{d}V - \int_{S_m} \boldsymbol{N}_S^T \bar{\boldsymbol{m}}\, J_{dS}\,\mathrm{d}S\right]$$
$$+ (\delta s)\left[\int_V \left(\boldsymbol{B}_{\boldsymbol{curl}}\hat{\boldsymbol{u}} - 2\boldsymbol{N}\hat{\boldsymbol{\omega}}\right) J_d \,\mathrm{d}V\right] = 0, \tag{60}$$

where J_d and J_{dS} represent the determinants of the Jacobian of the volume and the surface of an element, respectively. For the integration over the 8-noded isoparametric couple-stress elements presented here, standard 3×3 point Gauss quadrature is used [20,21].

Due to the fact that the variational factors, $\delta\hat{\boldsymbol{u}}$, $\delta\hat{\boldsymbol{\omega}}$, and $\delta\boldsymbol{s}$ have arbitrary value, the three terms in square brackets above all must be identically zero for this equation to be valid. This provides us with three coupled sets of linear algebraic equations for each element. These are our final individual finite element equations in matrix form.

We have now a set of linear algebraic equations for each element. Here, we choose to organize these element equations into the standard form shown in Fig. 2.

The stiffness terms on the left-hand side are calculated as follows:

$$\boldsymbol{K_u} = \int_V \left(\boldsymbol{B}_{\boldsymbol{e}}^T \boldsymbol{c}\boldsymbol{B}_{\boldsymbol{e}}\right) J_d \mathrm{d}V, \tag{61a}$$

$$\boldsymbol{K}_\omega = \int_V (\boldsymbol{B}_{\boldsymbol{k}}^T \boldsymbol{b}\boldsymbol{B}_{\boldsymbol{k}}) J_d \mathrm{d}V, \tag{61b}$$

$$\boldsymbol{K_{curl,s}} = \int_V (\boldsymbol{B_{curl}})\, J_d \mathrm{d}V, \tag{61c}$$

$$\boldsymbol{K_{\omega,s}} = \int_V (-2\boldsymbol{N})\, J_d \mathrm{d}V. \tag{61d}$$

For the right-hand side, we have

$$\hat{\boldsymbol{f}}_{\boldsymbol{x}} = \int_V \boldsymbol{N}^T \bar{F}_x J_d \, \mathrm{d}V + \int_{S_t} \boldsymbol{N}_S^T \bar{t}_x J_{dS} \mathrm{d}S, \tag{62a}$$

$$\hat{\boldsymbol{f}}_{\boldsymbol{y}} = \int_V \boldsymbol{N}^T \bar{F}_y J_d \, \mathrm{d}V + \int_{S_t} \boldsymbol{N}_S^T \bar{t}_y J_{dS} \, \mathrm{d}S, \tag{62b}$$

$$\hat{\boldsymbol{m}} = \int_{S_m} \boldsymbol{N}_S^T \bar{m} \, J_{dS} \, \mathrm{d}S, \tag{62c}$$

where the subscripts x and y above indicate the components of force and traction in that respective direction. All terms that appear in the right-hand side are of course known quantities.

After evaluating the stiffness matrix and forcing vector on the element level, we then follow standard finite element procedures to assemble and solve the global set of linear algebraic equations

$$\boldsymbol{K}\boldsymbol{u} = \boldsymbol{f}, \tag{63}$$

where now $\boldsymbol{u}$ includes displacements, rotations, and skew-symmetric stresses.

Before examining several applications of the consistent couple stress FE formulation in the next section, a simple patch test is performed to show that indeed the elements used here are viable. Consider the performance of the square mesh with distorted elements shown in Fig. 3 with material parameters $E = 5/2$, $\nu = 1/4$ and $l = 1$. First, the displacement boundary conditions corresponding to rigid body states are imposed on the edge nodes of the patch. Thus, displacement boundary conditions are enforced at every boundary node corresponding to a unit rigid body translation in the x- and y-directions. This of course should result in zero stress and strain within the body for both cases. The error in the resulting stress and strain fields was less than 10^{-14}. Next, displacement boundary conditions corresponding to a constant rotation state were enforced by specifying boundary conditions, such that $\omega = (u_{y,x} - u_{x,y})/2 = 1$. Again, the error in the resulting stress and strain fields was less than 10^{-14}. Finally, a constant strain and stress state was enforced on all edges of the mesh in Fig. 3. The specific conditions were defined for a stress state with $\sigma_{xx} = 2$ and $\sigma_{yy} = \sigma_{xy} = 0$ to exist everywhere within the body. The resulting stress and strain fields from enforcing the boundary conditions compatible with this constant strain and stress state were accurate everywhere in the body to within machine precision. More specifically, the maximum values of error for all stresses and strains, when compared to the analytical solution, were less than 10^{-14}.

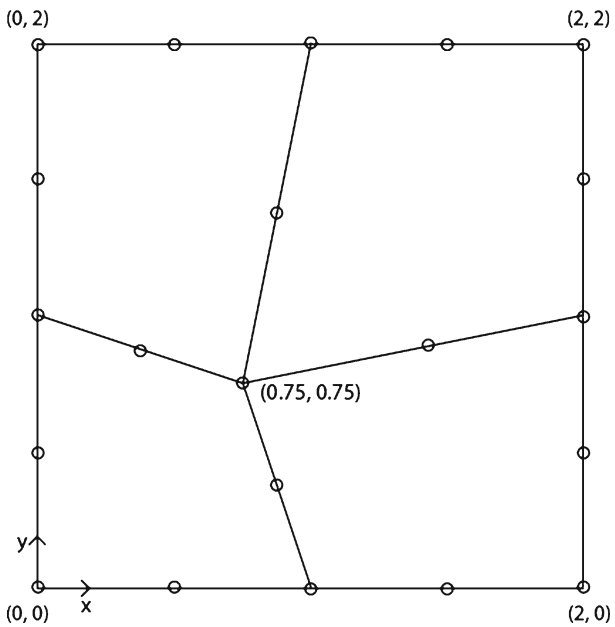

Fig. 3 Mesh used for patch test

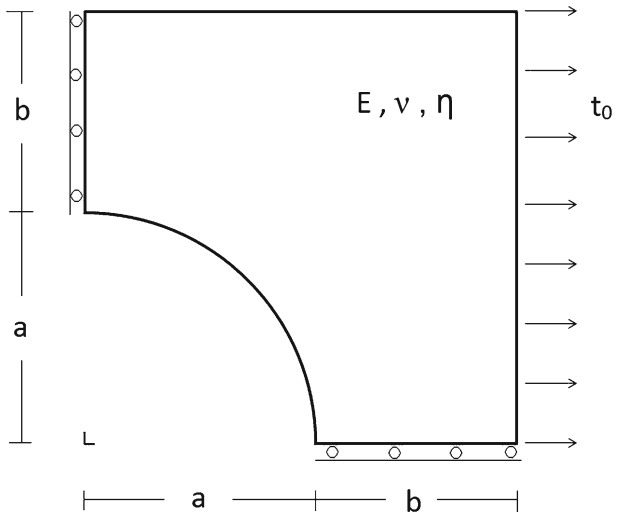

Fig. 4 Problem schematic of hole in finite plate

Table 1 Results for hole in a finite plate

	$\frac{l^2}{a^2}$	BEM 160 elements	FEM 12 elements	FEM 133 elements	FEM 841 elements
U_{CL}	1.00E-08	1.4634	1.4436	1.4615	1.4634
	0.0625	0.9387	0.9527	0.9362	0.9388
	0.25	0.7051	0.7133	0.7030	0.7051
	1	0.6038	0.6091	0.6022	0.6039
U_{TC}	1.00E-08	0.1464	0.1493	0.1465	0.1464
	0.0625	0.3557	0.3547	0.3559	0.3557
	0.25	0.4617	0.4646	0.4619	0.4617
	1	0.5102	0.5158	0.5102	0.5102
SCF	1.00E-08	3.1935	3.1073	3.2080	3.1948
	0.0625	2.0058	1.9438	2.0165	2.0056
	0.25	1.4998	1.4360	1.5072	1.5000
	1	1.2866	1.2265	1.2931	1.2869

5 Size-dependent elasticity problems

5.1 Uniform traction on plate with circular hole

The first example we consider is that of a circular hole in a plate using plane-strain assumptions. Previously, Mindlin [23] studied stress concentration factors for this problem within the inconsistent couple stress theory.

Symmetry considerations allow us to simplify the problem geometry to a quarter plate, as shown in Fig. 4. We consider dimensions $a = b = 1$ and uniform traction, $t_0 = 1/2$. The material properties are taken in non-dimensional form, as $E = 5/2$ and $\nu = 1/4$, to provide a shear modulus of unity.

Referring to Fig. 4, the boundary conditions for this problem are as follows. The top surface and the circular surface are both traction-free. The left surface has zero horizontal displacement, zero vertical traction, and zero rotation. The bottom surface has zero vertical displacement, zero horizontal traction, and zero rotation, whereas the right side is subject to uniform horizontal traction t_0.

The results are tabulated for various values of the couple stress parameter, η, which in this case is equal to l^2/a^2, in Table 1. Increasing values of l^2/a^2 can be seen as decreasing the characteristic geometry of the problem. Here, $\mathrm{U_{CL}}$ is the horizontal displacement at the centerline, or the bottom right corner in Fig. 4, $\mathrm{U_{TC}}$ is the horizontal displacement at the top right corner, and SCF is the stress concentration factor for this structure at the top of the hole. We see that these results are in excellent agreement with the boundary element results from [22].

For this problem, the smallest value of $l^2/a^2 = 1 \times 10^{-8}$ essentially yields the same solution as the classical plane-strain solution. We see that by increasing this parameter, the effect of including couple-stress

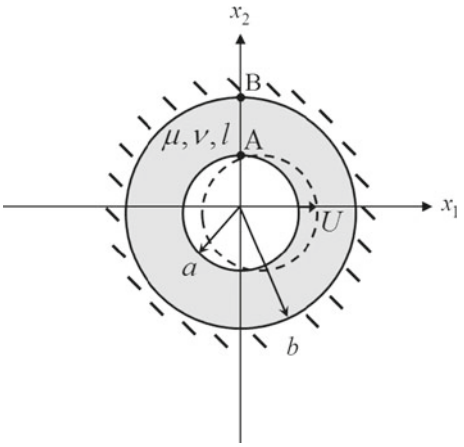

Fig. 5 Problem schematic of planar deformation of ring

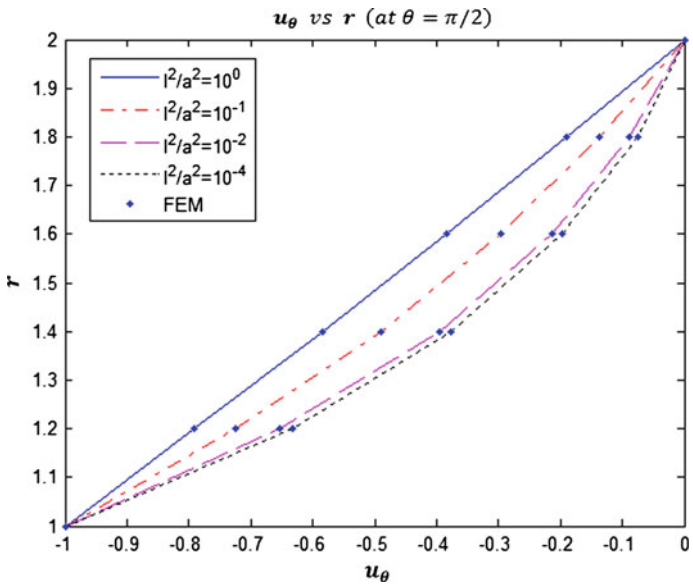

Fig. 6 Plot of u_θ for analytical and FEM solutions along center line $\theta = \pi/2$

effects causes significant deviation from the classical solution. Most interesting is the sharp decrease in the stress concentration factor with increasing value of the couple stress parameter.

5.2 Deformation of a plane ring

The second example considered is the deformation of a ring, as shown in Fig. 5, using plane-strain assumptions. The deformation is a unit displacement of the inner surface in the positive x-direction. Again for material properties, we use $E = 5/2$ and $\nu = 1/4$. The inner surface has radius $a = 1$, and the outer surface has radius $b = 2$. Point A is located at $r = a$ and $\theta = \pi/2$, while Point B is located at $r = b$ and $\theta = \pi/2$.

The boundary conditions are as follows: On the outer surface, we have zero displacement, while on the inner surface, a unit horizontal displacement ($U = 1$) is enforced as well as zero vertical displacement. There are no applied tractions or body forces.

There is an analytical solution available for this particular problem from [11]. For the finite element analysis, an unstructured mesh consisting of 2,900 elements was used with refinement about point A. Figures 6 and 7 compare the present finite element solutions for u_θ and ω, respectively, with the corresponding analytical results, while the force-tractions at A and B are provided in Table 2. All of the finite element solutions are in excellent agreement with the analytical solutions.

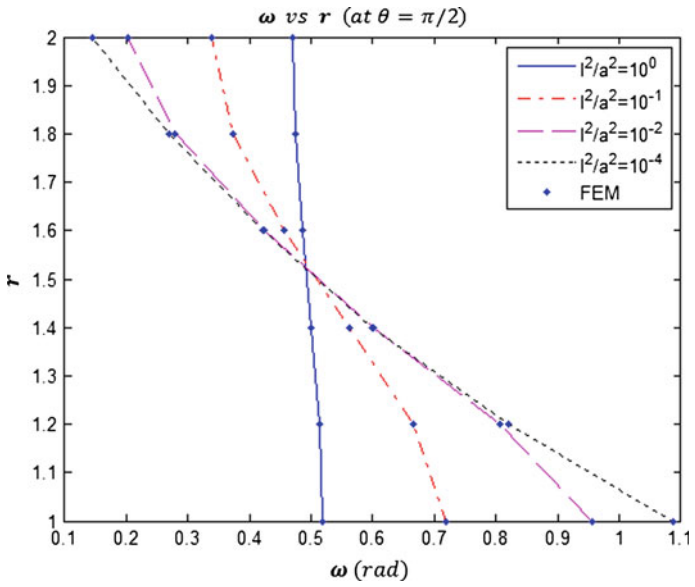

Fig. 7 Plot of ω for analytical and FEM solutions along center line $\theta = \pi/2$

Table 2 Results for tractions at points A and B

$\frac{l^2}{a^2}$	$t_\theta(A)$			$t_\theta(B)$		
	Analytical	FE	Error	Analytical	FE	Error
10^{-4}	−2.2096	−2.2095	4.53E-05	0.27614	0.27612	7.24E-05
10^{-2}	−2.2285	−2.2280	2.24E-04	0.2744	0.2744	1.82E-04
10^{-1}	−2.3310	−2.3312	8.58E-05	0.2880	0.2881	1.74E-04
10^{0}	−2.8192	−2.8255	2.23E-03	0.6682	0.6677	7.48E-04

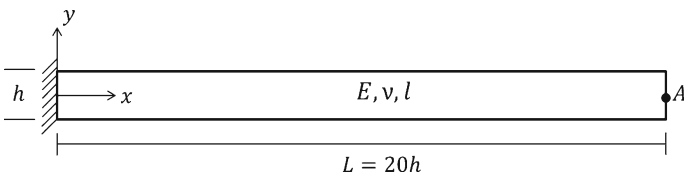

Fig. 8 Schematic of cantilever

5.3 Transverse plane-strain deformation of a cantilever

The final problem considered is the transverse deformation of a cantilever under plane-strain conditions, including couple-stress effects. This problem, which has no existing analytical solution, is illustrated in Fig. 8. An enforced displacement in the vertical direction is applied to the right end of the cantilever. For material properties, we use $E = 2$ and $\nu = 0$ to provide a unit shear modulus and to allow for comparison with elementary theory for limiting values of the couple stress parameter l. The cantilever has height, h, which we consider to be the characteristic dimension for the problem. Meanwhile, for the length, we assume two different values; $L = 20h$ and $L = 40h$ to assure that under classical theory bending deformation will dominate for both aspect ratios.

Two sets of boundary conditions also are considered. For Case 1, the boundary conditions are as follows: on the left end, zero displacement is enforced, while a unit vertical displacement is enforced on the right end. For Case 2, the rotations at the left end also are restrained to zero. In both cases, there are no applied force- and moment-tractions, and no applied body forces.

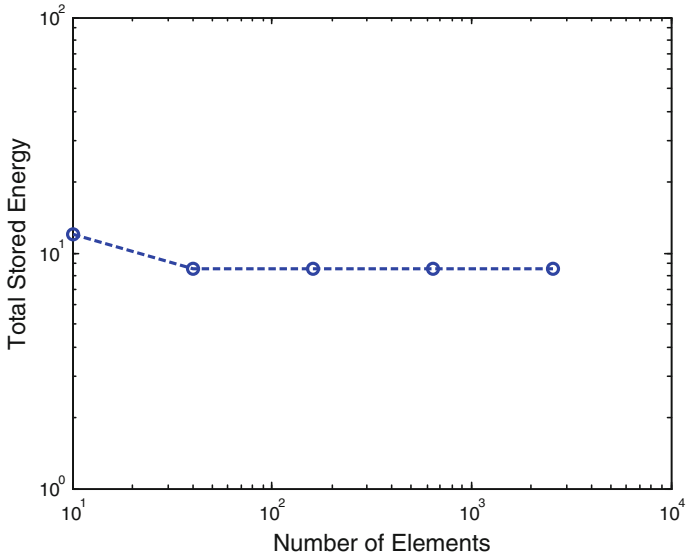

Fig. 9 Convergence of cantilever stored energy with mesh refinement

The mesh used here consists of rectangular elements arranged such that there are $20N$ elements lengthwise and $2N$ elements transversely. The finest mesh had $N = 8$ and therefore consisted of 2,560 elements. Figure 9 shows excellent convergence of the total stored energy with uniform mesh refinement for Case 1 with $L = 20h$ and $h/l = 1$. For the remainder of these numerical experiments, the characteristic geometric length scale, h, is altered, while the material parameters are held constant. This is used to investigate the size-dependency inherent in the consistent couple-stress theory. Specifically, the stiffness of the beam, K, is of great interest, which is equal to the vertical reaction force divided by the vertical displacement at point A. Figure 10a, b show the behavior of non-dimensional stiffness for Cases 1 and 2 of this length-scaling experiment. Meanwhile, Fig. 11 presents the deformed geometry of the cantilever with free rotations at the left end and $L = 20h$ for three distinct values of h/l.

From Fig. 10a, b, we can clearly see three well-defined domains associated with characteristic problem geometry. For large scale problems, where the characteristic geometry, h, is much greater than l, we have the classical elasticity region with stiffness independent of length scale. In this domain, couple-stress effects are negligible, mainly due to the small magnitude of curvature deformation at this scale. Notice that stiffness is equal to $3EI/L^3$ in this region, as expected from classical beam theory.

When the characteristic geometry for this problem is on the order of l, we enter the transitional couple-stress domain. For this cantilever problem, it is clear from Fig. 10a, b that couple-stress effects become significant for characteristic geometry of $h/l \approx 10$. In this couple-stress domain, there is an increase in flexural stiffness, which we see can have a significant effect on the overall effective stiffness of the body.

Finally, for very small values of h/l, we have a domain that is couple-stress "saturated" in both Fig. 10a, b. In other words, the flexural stiffness due to couple-stress effects has increased to the level where bending is suppressed, while shear deformation combined with rotation dominates. The absence of bending is clearly visible in the plot of deformed shape for $h/l = 0.0001$ in Fig. 11. Furthermore, from Fig. 10a, we find that for this particular problem, for sufficiently small h/l ratio, an increase in total stiffness by factors of 30 and 60 can be the result of including couple-stress effects with $L = 20h$ and $L = 40h$, respectively. In Case 2, where the rotational degree of freedom at the left-hand end is set to zero in the couple stress formulation, an even more dramatic increase in stiffness is seen, corresponding very nearly to pure shear deformation of the beam. As a result, for this couple stress "saturated" domain in Case 2, we find $K \propto GA/L$. Meanwhile, for the corresponding domain in Case 1, the stiffness scales with $1/L^2$.

For the length scales defined in Fig. 10a, b, the saturated couple-stress region corresponds to a maximum possible stiffness for a given problem geometry and loading. Whether this totally saturated couple-stress region can occur in physical systems is undetermined at this point. Physical experimentation with the goal of testing for the couple-stress material property η or l is necessary to know exactly what portions of these couple-stress domains are physically realizable.

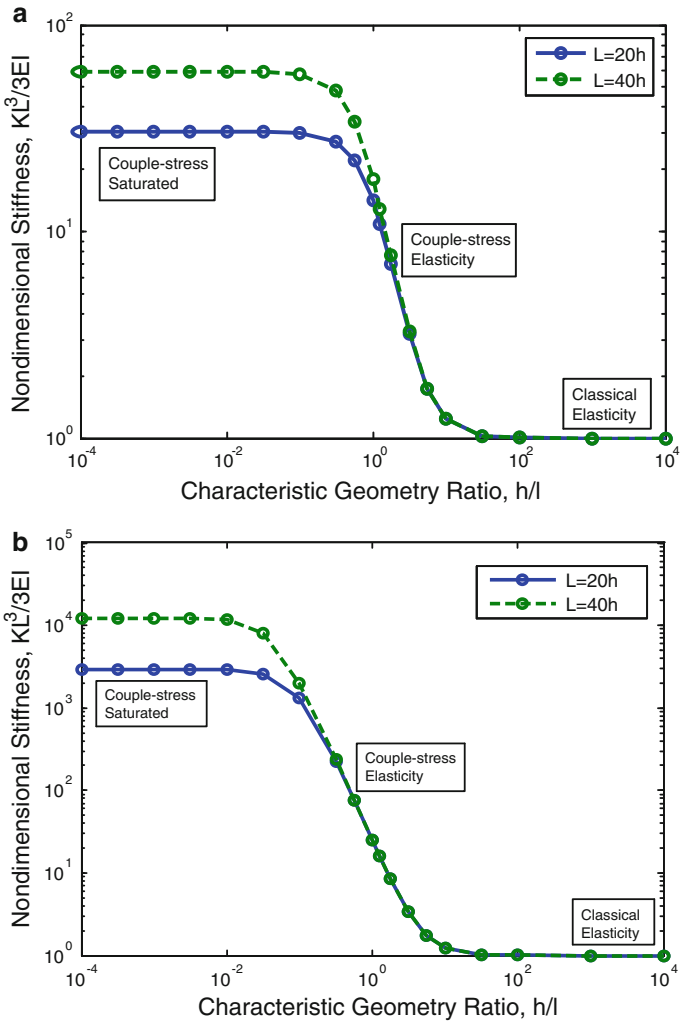

Fig. 10 Non-dimensional size-dependency of cantilever stiffness. **a** Case 1: $m = 0$ boundary condition at $x = 0$, **b** case 2: $\omega = 0$ boundary condition at $x = 0$

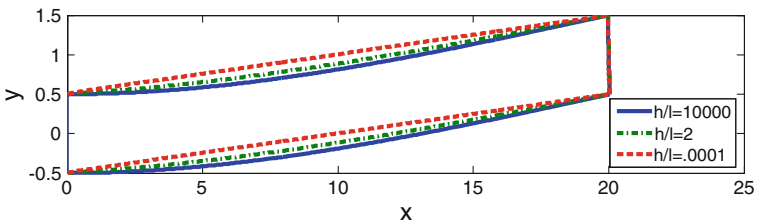

Fig. 11 Deformation of cantilever with $L = 20h$ and $m = 0$ boundary condition at $x = 0$ for select values of h/l

6 Conclusions

Based on the new consistent couple-stress theory for solids [11], we have developed a corresponding mixed variational principle and finite element formulation. The formulation presented here considers the rotation field to be separate from the displacement field in the underlying energy statement and then enforces rotation-displacement compatibility via Lagrange multipliers. This is a particularly attractive formulation because the Lagrange multipliers are directly related to the skew-symmetric portion of the stress tensor, which otherwise can be difficult to calculate accurately. Also, the engineering mean curvature vector was defined here and is shown to be the correct energy conjugate deformation vector to the couple-stress vector.

The finite element formulation was then employed to study several problems involving couple-stress phenomena with great accuracy in comparison with both analytical solutions and boundary element analysis. The final numerical experiment in Sect. 5 showed the size-dependency of couple-stress theory and highlighted three distinct length-scale domains, namely the classical elasticity domain, the transitional couple-stress domain, and the saturated couple-stress domain. Inclusion of the couple-stress effect was shown to cause potentially large increases in stiffness. Although here we only highlight this transition to shear dominated response for a simple cantilever, this phenomenon surely is a more general consequence of the consistent couple stress size-dependent mechanics theory.

With the exponentially increasing amount of technology that is being developed on the micro- and nano-scales, the need for tools to analyze size-dependent continuum mechanics problems is greater than ever. Here, we have presented a simple, robust, and highly accurate finite element formulation that is based on the consistent couple-stress theory and can be used to model linear elasticity problems on very fine length scales. The extensions to axisymmetric and three-dimensional problems are certainly of interest, as is the extension to inelastic response. Perhaps more important though is the need to investigate the predicted effects of couple stress theory through a rigorous program of physical experiments.

Acknowledgments This paper is based upon work by the first author supported by the US National Science Foundation (NSF) Graduate Research Fellowship under Grant Number 1010210. The authors also gratefully acknowledge support from NSF under Grant Number 0836768. The results presented here express the opinion of the authors and not necessarily that of the sponsor.

References

1. Voigt W.: Theoretische Studien über die Elastizitätsverhältnisse der Kristalle (Theoretical studies on the elasticity relationships of crystals). Abhandlungen der Gesellschaft der Wissenschaften zu Göttingen **34** (1887)
2. Cosserat, E., Cosserat, F.: Théorie des corps déformables (Theory of deformable bodies). A. Hermann et Fils, Paris (1909)
3. Toupin, R.A.: Elastic materials with couple-stresses. Arch. Ration. Mech. Anal. **11**, 385–414 (1962)
4. Mindlin, R.D., Tiersten, H.F.: Effects of couple-stresses in linear elasticity. Arch. Ration. Mech. Anal. **11**, 415–448 (1962)
5. Koiter, W.T.: Couple stresses in the theory of elasticity, I and II. In: Proceedings of the Koninklijke Nederlandse Akademie van Wetenschappen. Series B. Physical Sciences, vol. 67, pp. 17–44 (1964)
6. Mindlin, R.D.: Second gradient of strain and surface-tension in linear elasticity. Int. J. Solids Struct. **1**, 417–438 (1965)
7. Mindlin, R.D., Eshel, N.N.: On first strain-gradient theories in linear elasticity. Int. J. Solids Struct. **4**, 109–124 (1968)
8. Eringen, A.C., Suhubi, E.S.: Nonlinear theory of simple micro-elastic solids—I. Int. J. Solids Struct. **2**, 189–203 (1968)
9. Eringen, A.C.: Theory of micropolar elasticity. In: Liebowitz, H. (ed.) Fracture, vol. 2, pp. 662–729. Academic Press, New York (1968)
10. Nowacki, W.: Theory of Asymmetric Elasticity. Pergamon Press, Oxford (1986)
11. Hadjesfandiari, A.R., Dargush, G.F.: Couple stress theory for solids. Int. J. Solids Struct. **48**, 2496–2510 (2011)
12. Hadjesfandiari, A.R., Dargush, G.F.: Fundamental solutions for isotropic size-dependent couple stress elasticity. Int. J. Solids Struct. **50**, 1253–1265 (2013)
13. Hadjesfandiari, A. R.: On the skew-symmetric character of the couple-stress tensor. arXiv:1303.3569 (2013)
14. Herrmann, L.R.: Mixed finite elements for couple-stress analysis. In: Proceedings of the International Symposium on Hybrid and Mixed Finite Element Methods, Atlanta (1983)
15. Wood, R.D.: Finite element analysis of plane couple-stress problems using first order stress functions. Int. J. Numer. Methods Eng. **26**, 489–509 (1988)
16. Providas, E., Kattis, M.A.: Finite element method for plane Cosserat elasticity. Comput. Struct. **80**, 2059–2069 (2002)
17. Padovan, J.: Applications of 3-d finite element procedures to static and dynamic problems in micropolar elasticity. Comput. Struct. **8**, 231–236 (1978)
18. Shu, J.Y., King, W.E., Fleck, N.A.: Finite elements for materials with strain gradient effects. Int. J. Numer. Methods Eng. **44**, 373–391 (1999)
19. Amanatidou, E., Aravas, N.: Mixed finite element formulations of strain-gradient elasticity problems. Comput. Methods Appl. Mech. Eng. **191**, 1723–1751 (2001)
20. Zienkiewicz, O.C., Taylor, R.L.: The Finite Element Method. Butterworth-Heinemann, Oxford (2000)
21. Bathe, K.J.: Finite Element Procedures. Prentice Hall, New Jersey (2006)
22. Hadjesfandiari, A.R., Dargush, G.F.: Boundary element formulation for plane problems in couple stress elasticity. Int. J. Numer. Methods Eng. **89**, 618–636 (2011)
23. Mindlin, R.D.: Influence of couple-stresses on stress concentration. Exp. Mech. **3**, 1–7 (1963)